JAERI- M
5877

FACTORS INFLUENCING THE YOUNG'S MODULI OF COMPACT MATRICES AND FUEL COMPACTS FOR HTGR FUEL

October 1974

Akira KIKUCHI and Kazumi IWAMOTO

日本原子力研究所
Japan Atomic Energy Research Institute

この報告書は，日本原子力研究所がJAERI-Mレポートとして，不定期に刊行している研究報告書です．入手，複製などのお問合わせは，日本原子力研究所技術情報部（茨城県那珂郡東海村）あて，お申しこしください．

JAERI-M reports, issued irregularly, describe the results of research works carried out in JAERI. Inquiries about the availability of reports and their reproduction should be addressed to Division of Technical Information, Japan Atomic Energy Research Institute, Tokai-mura, Naka-gun, Ibaraki-ken, Japan.

JAERI-M 5877

Factors Influencing the Youngs Moduli of Compact Matrices and Fuel Compacts for HTGR Fuel

Akira KIKUCHI and Kazumi IWAMOTO
Division of Nuclear Fuel Research, Tokai, JAERI

(Received October 3, 1974)

By an ultrasonic propagation procedure, the Young's moduli of fuel compacts and compact matrixes were measured at room temperature. On the other hand, the density and orientation of the matrixes and the crystallite sizes of the graphite powders were determined to characterize the samples.

The Young's modulus increases with content of the amorphous carbon and decreases with increase of the natural graphite in the sample (PCG-NG system). The propagation velocity from which the Young's modulus is calculated depends on the density and orientation in anisotropic samples (NCG system), while it depends only on the density in isotropic samples (MICG system).

JAERI-M 5877

HTGR燃料用コンパクトマトリックスおよび燃料コンパクトのヤング率に影きょうを及ぼす諸因子

日本原子力研究所東海研究所燃料工学部

菊地　章・岩本多実

（1974年10月3日受理）

燃料コンパクトおよびコンパクトマトリックスのヤング率が，超音波伝播法により，室温で測定された。1方，コンパクトマトリックスの密度と配向性および黒鉛粉末の結晶子径が実験用試料を特性づけるために求められた。

ヤング率は無定形炭素の含有量とともに増大し，混合黒鉛系PCG-NGでは天然黒鉛の量が増すにつれて減少する。ヤング率の計算で用いる伝播速度は，異方性試料では密度および配向性に依存するが，等方性試料では密度のみに依存することが判った。

目　次　な　し

I Introduction

Fuel bodies for HTGR are normally made by incorporating pyrocarbon-coated fuel particles with graphite powder and resin binder in cylindrical or spherical shape. In the case of fuel compact, the coated particles are overcoated with graphite powder/resin binder to have their uniform distribution and the mixture is pressed with a die into compact, followed by heat-treatment to cure and carbonize the graphite resin matrix.

The matrix of graphite needs to have good thermal conductivity, to provide local mechanical support for the particles, to withstand internal thermal and irradiation induced dimensional changes and stresses without disintegration, and to act as a chemical passive for fission products emmited from the coated particles. As reported by W.W.Delle et al.[1] and M.Hrovat et al.[2], the subject of research and developement for the compact matrix is to find an adequate material having these properties necessary for the fuel compact.

In contrast with usual materials, the mechanical properties of graphite are sensitive to such as the size and alinement of graphite crystallites. The mechanical properties of the compact matrix thus depends on the properties of graphite powder, density, orientation and amorphous carbon-quantity, as seen in Fig.1, which shows the constitution of fuel compact and the respective characteristics influencing the properties of the compact matrix. The Young's modulus, in addition to the matrix density, of the

fuel compact or compact matrix is reported to be applied as an inspection method[3] of the quality of fuel body for HTGR. The Young's modulus of compact matrix mainly depends on the graphite filler. Basic studies on the Young's modulus of graphite were made by R.H.Knibbs[4], J.H.W.Simmons[5], C.Baker et al.[6] and R.J.Price[7]. However, the Young's modulus of compact matrix is not clarified yet especially concerning the matrix density and graphite orientation.

In the present work, the Young's moduli of several types of the compact matrixes and also some fuel compacts were measured at room temperature by an ultrasonic propagation method to observe the dependence of the moduli upon the density and orientation of matrix. To characterize the graphite powder, the crystallite sizes were determined by X ray diffraction analysis, and the size and shape of the powder were observed by SEM analysis.

II Experimental

2.1 Samples

2.1.1 Characteristics of graphite powder

Characteristics of the graphite powder-MICG (Milled Isotropic Coke Graphite), NCG (Needle Coke Graphite) and PCG (Petroleum Coke Graphite)-used in fabrication of the experimental samples will first be described. The shape and size of graphite powder were confirmed by a scanning electron microscope (SEM). As seen in Photo 1, there are distinct differences

in shape between the graphite powders. X ray diffraction analysis was made to obtain the crystallite sizes. In Table 1, the sizes Lc(002) and La(110) are shown together with the intensity ratio S(004)/S(110) determined from the diffraction patterns in Fig.2 . The NCG powder has the crystallite structure growing in a-axial direction while the MICG has nearly the same size of crystallite in both a- and c-directions, and the PCG has relatively large isotropic crystallites.

2.1.2 Compact matrix and fuel compact

The samples used are the compact matrix and fuel compact, as shown in Table 2. The four kinds of graphite powder and three different binder contents were chosen as parameters for fabrication of the samples. The compact matrixes were prepared as follows. After mixing the graphite powder with phenol resin binder and alcohol, the mixture was dried in a vacuum and pulverized, then granulated in a rotating drum to have the suitable size corresponding to that of overcoated particles for fabrication into the fuel compact. These particles were warm-presssed into a cylindrical form under the pressure of 50 to 300 kg/cm^2 at 100 to 250 °C by an axial pressing. The pressed body was heat-treated for carbonization at 800 °C for 2 hr, and finally heated for degassing at 1800 °C for 1 hr in the vacuum of about 10^{-4} to 10^{-3} mmHg. In the case of fuel compact, the overcoating of graphite powder/resin binder mixture is first made to the TRISO-II type coated particles, and then the overcoated particles are pressed, followed by the procedure described. Concerning the amount of amorphous carbon formed by decomposition of the binder,

carbonization experiment of the binder indicated that about 50 % of amorphous carbon had left in the sample. Microphotographs of the typical compact matrixes (M2, M4 and M6) are shown in Photo 2; differences in the structures are seen. Moreover, SEM observations of the fractured faces ($\perp$ and // planes) for the compact matrixes (M2 and M4) are shown in Photo 3. Differences with the planes are evident.

2.2 Experimental apparatus and procedure

2.2.1 Young's modulus and Poissons ratio

The Young's modulus and Poissons ratio were measured by an ultrasoniscope (MIN-1105, Marui Co. Ltd.) using $BaTiO_3$ oscillators, and the propagation time through the sample was measured. The experimental apparatus used is shown in Photo4.

The Young's modulus (E) was calculated from the density (ρ), propagation velocity (V) and Poissons ratio (ν) with a longitudinal wave :

$$E = \rho V^2 \frac{(1+\nu)(1-2\nu)}{(1-\nu)} \qquad (1)$$

The Poissons ratio was measured from the propagation velocities of longitudinal and side waves (Vl and Vs) by the following equation ;

$$\nu = \frac{Vl^2 - 2Vs^2}{2(Vl^2 - Vs^2)} \qquad (2)$$

The standard deviation for measurements of the propagation time was about 0.1 μsec in each sample for the five times of measure-

ment.

2.2.2 Graphite orientation in the compact matrixes

The orientation of a graphite is usually estimated by X ray diffraction. The method, however, can not be applied to the fuel compact since the matrix portion of the fuel compact is too small to give a matrix specimen for exposure to the X rays. Therefore, a polarized light reflection method was used for obtaining the graphite orientation considering the application to fuel compact in future. The sample was polished with emery papers (5 minutes each with #400, #800 and #1200) and with diamond pastes (each 20 minutes with #A and #C), and then the polished sample was set on the rotating sample stage of the polarized light-microscope (Carlzeiss Jena Co. Ltd., East Germany). The reflective intensity of the light from the surface was measured by the Microscope Universal Exposuremeter (Olympus Co. Ltd.) for a rotating angle. An example of the intensity change with angle is shown in Fig.3 . In the figure, strangely there is no symmetry around 180°, for which the cause is not clear yet. In the present study, the reflective intensity ratio (IR) is used to express the orientation, defined as

$$IR = r_x / r_z \qquad (3)$$

where r_x and r_z are the maximum and minimum intensities at 0° and 90° , respectively. The IR values measured for typical samples are shown in Table 3 together with the data for pure graphites. The values of BAF, for reference, were calculated

with the equations[8] on the note *4 in the table. The planes (⊥ and //) and also the measuring directions for Young's modulus are indicated in Fig.4 .

In addition, to reconfirm in this respect, X ray diffraction analysis was made on the fractured face of the compact matrix. The diffraction patterns are shown in Fig.5, where the (004) and the (110) peaks are compared. In the figure, it is seen that the prefered orientation of a-basal plane is in the parallel with the pressing direction (see Fig.4), as indicated by the data (M4//) of intensity ratio IR in Table 3.

2.2.3 Density

Bulk density was calculated from the dimention and weight of the test specimen.

III Results and discussion

3.1 The effect of coated particles and amorphous carbon on the Young's modulus

The Young's moduli of fuel compacts and compact matrixes are shown in Fig.6 . In all the samples, the Young's modulus increases with increase of the binder content. This is easily explained by the fact that the Young's modulus of amorphous carbon is generally larger than that of polycrystalline graphite , because the Young's modulus of the carbon is nearly equal to that in a-axial direction (a-basal plane) of graphite single crystal[9]. It is to be noted that the Young's modulus in sample M4⊥ is much larger than that of M4 // , and those in M2⊥ and M6⊥

are not so large compared with those of M2// and M6// , respectively. These phenomena just fit to the data of orientation in Table 3. It thus appears that the orientation is an important factor in the Young's modulus.

The Young's modulus of fuel compact is larger than that of compact matrix as shown in the figure, possibly because of existence of the coated particle.

3.2 The effect of natural graphite added to petroleum coke graphite (PCG-NG mixing system) on the Young's modulus

The mixing effect of natural graphite mixed with PCG on the Young's modulus is indicated in Fig.7 . In both fuel compact and compact matrix, the Young's modulus decreases linearly with natural graphite content. It is probable caused by small Young's modulus of the natural graphite compared with the artificial one; the Young's modulus of graphite decreases generally with increase of the graphitization.

3.3 The effects of density and orientation on the Young's modulus and the propagation velocity

To observe the effects of density and orientation on the Young's modulus, two typical compact matrixes, i.e. M2 and M4 in Table 2, were chosen. One is the matrix composing of MICG and the other of NCG. As described already, the latter is strongly anisotropic and the former isotropic. Both the matrixes contain the same quantity of amorphous carbon. The samples, both M2 and M4, were cut into pieces, perpendicularly to the pressing direction (see Fig.4) with a diamond wheel cutter. These sliced specimens have different densities and orientations,

though composition of the matrix is the same. The density decreases gradually from one end to the other of the sample, as expected for a one-end pressed compact.

The Young's modulus versus density is shown in Figs.8 and 9 for M2 and M4, respectively. The curve for M2 is relatively simple whereas the one for M4 has a curvature in the vicinity of the density of about 1.57 g/cm^3. It should be noted, however, that the Young's modulus for M4 is larger than that for M2, despite the larger density of M2 than that of M4; there is some relation between Young's modulus and intensity ratio in the M4.

To see the respective contributions of density and orientation to the Young's modulus, it is necessary to consider the propagation velocity from which the Young's modulus is calculated (see Eq.1), because the equation contains the density term. The propagation velocity and the reflective intensity ratio versus density are shown in Fig.10 for both M2 and M4. In sample M2, the ratio is independent of the density within the IR-error of ± 0.02 at least, but the ratio in M4 increases with increase of the density. The simplicity of velocity curve in M2 is thus due to dependency of the velocity only on the density. In the sample M4, on the other hand, it is possible that the value of propagation velocity beyond about 3.25×10^5 cm/sec is the summation of contributions by the density and orientation, because the reflective intensity ratios in the region of density 1.52 to 1.57 g/cm^3 are constant within the standard deviation (IR = 1.10 ± 0.01), as seen in the upper figure on the right hand side. Consequently, the shadowed area in the figure is equivalent to

the increment due to intensity ratio.

Now, it is possible to separate the contributions of density and intensity ratio influencing the propagation velocity. Deducing from Fig.10, Figs.11 and 12 are obtained. In Fig.11, the difference of propagation velocity (ΔV) is plotted against the density difference ($\Delta\rho$) on logarithmic scale, in which the constants V_o and ρ_o are the values in the specimen having the lowest density. Points for each matrix are entirely on a linear line in both the matrixes. As seen in the figure, the results can be formulated in exponential function. In Fig.12, on the other hand, there is linearity between velocity difference (ΔV) and intensity ratio difference (ΔIR) only in the sample M4 and the relationship can be given in the linear function. The formulas are summarized as follows.

For the density dependency,

$$\Delta V = a(\Delta\rho)^n \tag{4}$$

$$\Delta V = V - V_o$$

$$\Delta\rho = \rho - \rho_o$$

where a and n are constants (a:2.14±0.02 and n:0.740 for M4, and a:1.44±0.07 and n:0.858 for M2), and V_o and ρ_o are initial values (V_o:3.02 and ρ_o:1.52 for M4, and V_o:2.40 and ρ_o:1.66 for M2).

For the orientation dependency,

$$\Delta V = b(\Delta IR) \tag{5}$$

$$\Delta V = V - V_o$$

$$\Delta IR = IR - IR_o$$

where b is a constant (b:2.00), and V_o and IR_o are initial values (V_o :3.24 and IR_o:1.11) in M4.

IV Conclusion

By an ultrasonic propagation procedure, the Young's moduli of fuel compacts and compact matrixes were measured at room temperature. In addition, the density and orientation of compact matrixes were determined to characterize the respective specimens. Furthermore, characteristics of the graphite powders constituting the samples were clarified by X ray diffraction analysis and SEM observation.

The followings were confirmed :

1) Amorphous carbon included in the sample as a component increases the Young's modulus in both fuel compact and compact matrix.
2) The Young's modulus of fuel compact is larger than that of compact matrix, if the matrix composition is the same.
3) The Young's modulus strongly depends on the graphite orientation. In the anisotropic sample, the Young's modulus differs largely due to the measuring directions.
4) The propagation velocity from which the Young's modulus is calculated is a function of the density and orientation. In the isotropic sample, the velocity depends only on the density, but in the anisotropic sample it depends both on the density and

orientation.

5) By analyzing the data obtained, the following equations are introduced for the contributions of density and orientation to the propagation velocity ;

$$V = V_o + a(\rho - \rho_o)^n$$

$$V = V_o' + b(IR - IR_o)$$

where ρ is the density, IR the reflective intensity ratio, and V_o, a, ρ_o, n, V_o', b and IR_o are the constants determined by characteristics of the sample, including the kind of graphite powder, crystallite size and its alinement and the fabrication conditions of sample.

Acknowledgement

The authers wish to express their thanks to Mr.T.Ishihara, Office of Planning, and Dr.S.Nomura, Chief of Division of Nuclear Fuel Research, for their encouragement, and also to Mr.T.Tobita for his assistance in the experiment.

References

(1) W.W.Delle et al., BNES Conf., 1973, London, P.27.1

(2) M.Hroval et al., Jül-969-RW (1973)

(3) J.Holliday et al., BNES Conf., 1973 London, P.13.1

(4) R.H.Knibbs, Carbon, 7, 225, (1969)

(5) J.H.N.Simmons, 3rd Conf. Carbon , 559 (1959) Pergamon

(6) C.Baker et al., Phil. Mag., 9, 927 (1964)

(7) R.J.Price, Phil. Mag., 12, 561 (1965)

(8) K.Koizlik, Jül-868-RW (1972)

(9) I.B.Mason et al., Carbon, 5, 493, (1967)

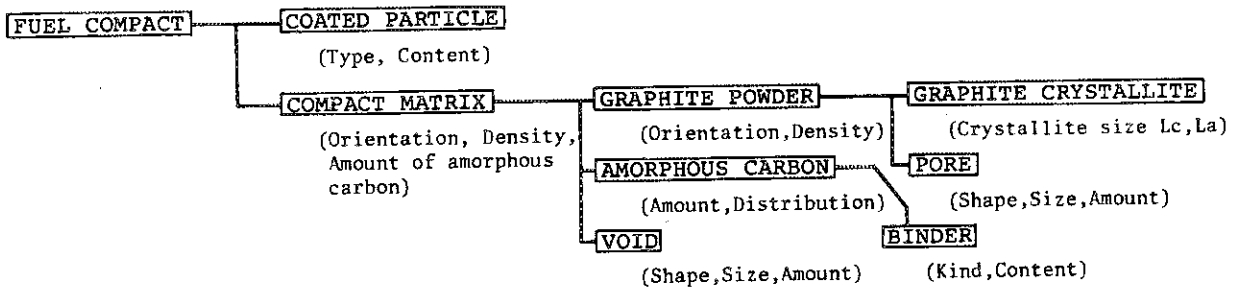

Fig./ Flow diagram of the constitution of fuel compact and the respective characteristics influencing the properties of compact matrix

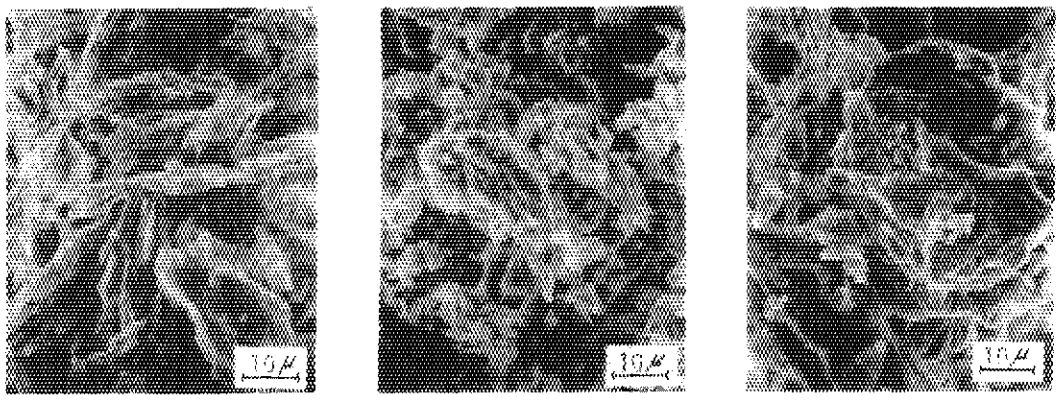

NCG Powder MICG Powder PCG Powder

Photo / The shape and size of graphite powders -NCG(Needle coke graphite), MICG(Milled isotropic coke graphite) and PCG(Petroleum coke graphite)- used in fabrication of the fuel compact and the compact matrix (Scanning electron microscope-observation)

Table 1 Characteristics of graphite powder used in the fabrication of experimental samples

Graphite powder*1	Crystallite size*2 Å		S(004)/S(110)*3
	Lc(002)	La(110)	
MICG	390	760	3.30
NCG	390	1900	20.07
PCG	1000	990	6.91

*1 MICG : Milled isotropic coke graphite
NCG : Needle coke graphite
PCG : Petroleum coke graphite

*2 X ray diffraction analysis with Si standard
X ray : Cupper Kα (Ni filter)
Slitt system : D.S. - S.S. - R.S.
(1/6)° - 0.15 - (1/6)° for (002)
4° - 0.30 - 4° for (110)

*3 Intensity ratios of diffraction peaks

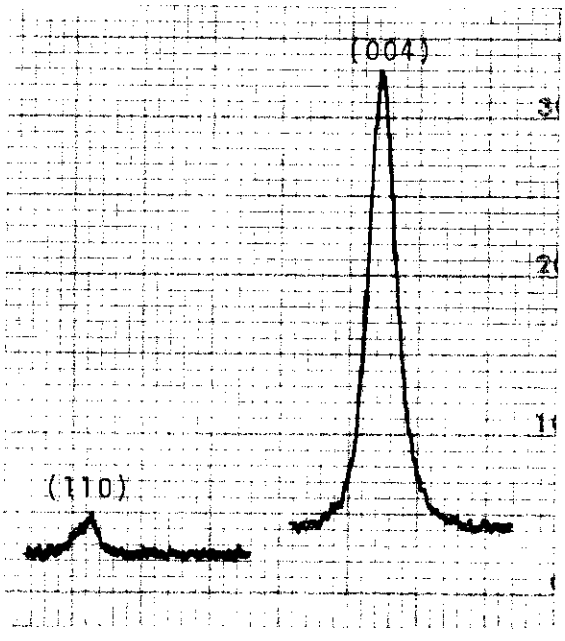

Needle coke graphite powder

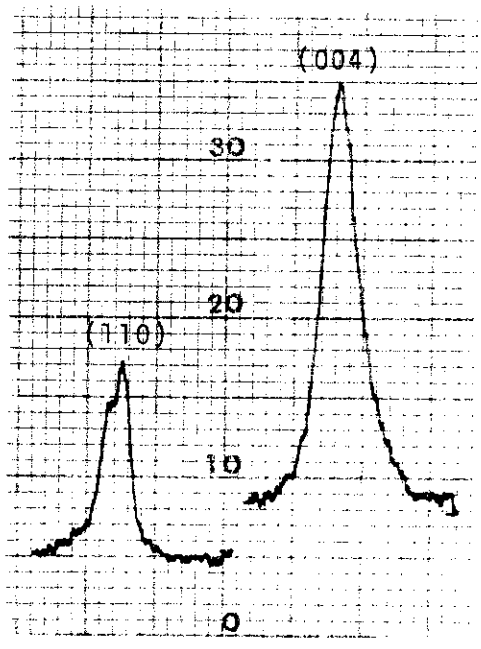

Milled isotropic coke graphite powder

Fig.2 Typical X ray diffraction patterns (110) and (004) in needle coke and milled isotropic coke graphite powders

Table 2 Compact matrices and fuel compacts used in the experiments

Sample *1	Sample No.	Graphite powder *3 used	Added *4 binder (%)	Apparent *5 density (g/cm^3)
Compact matrix	M1	MICG	10	1.63
	M2	MICG	20	1.66
	M3	NCG	10	1.66
	M4	NCG	20	1.58
	M5	PCG	10	1.63
	M6	PCG	20	1.66
	M7	0.9PCG-0.1NG	10	1.65
	M8	0.5PCG-0.5NG	10	1.60
	M9	0.2PCG-0.8Ng	10	1.62
Fuel *2 compact	F1	MICG	14	1.66
	F2	MICG	20	1.70
	F3	NCG	14	1.65
	F4	NCG	20	1.70
	F5	PCG	14	1.66
	F6	PCG	20	1.75
	F7	0.9PCG-0.1NG	14	1.65
	F8	0.5PCG-0.5NG	14	1.67
	F9	0.2PCG-0.8NG	14	1.66

*1 Fabricated by one side pressing under the pressure of 50 to 300 kg/cm^2

*2 Containning about 22 v/o of TRISO-11 type coated particles

*3 MICG : Milled isotropic coke graphite
NCG : Needle coke graphite
PCG : Petroleum coke graphite
NG : Natural graphite

*4 Phenol resin binder (Amorphous carbon content in the sample is about 50 %.)

*5 Calculated matrix density

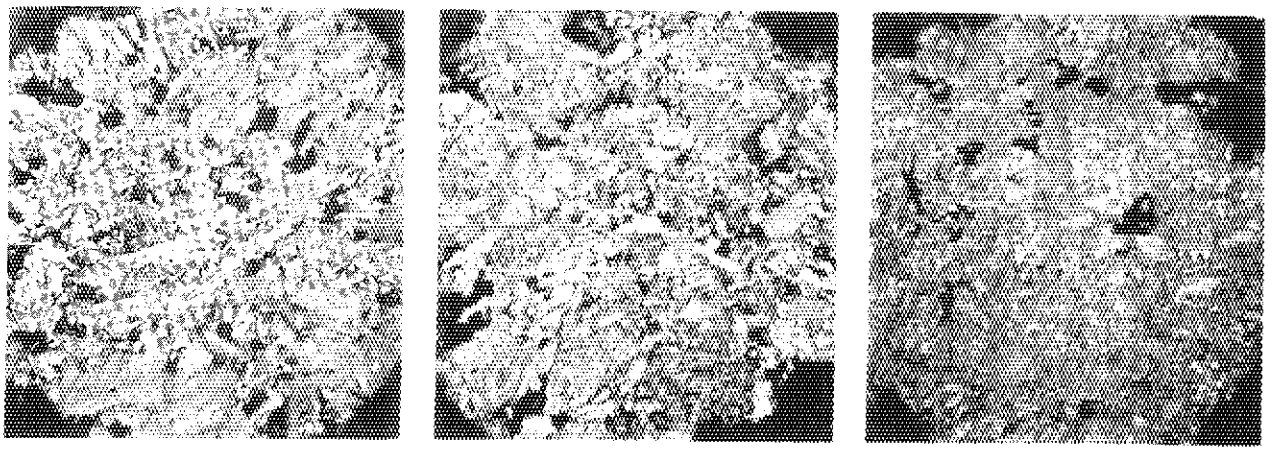

Sample M4 (NCG) Sample M2 (MICG) Sample M6 (PCG)

Photo 2 Structures of typical compact matrixes M4 (NCG-Needle coke graphite), M2 (MICG-Milled isotropic coke graphite) and M6 (PCG-Petroleum coke graphite)

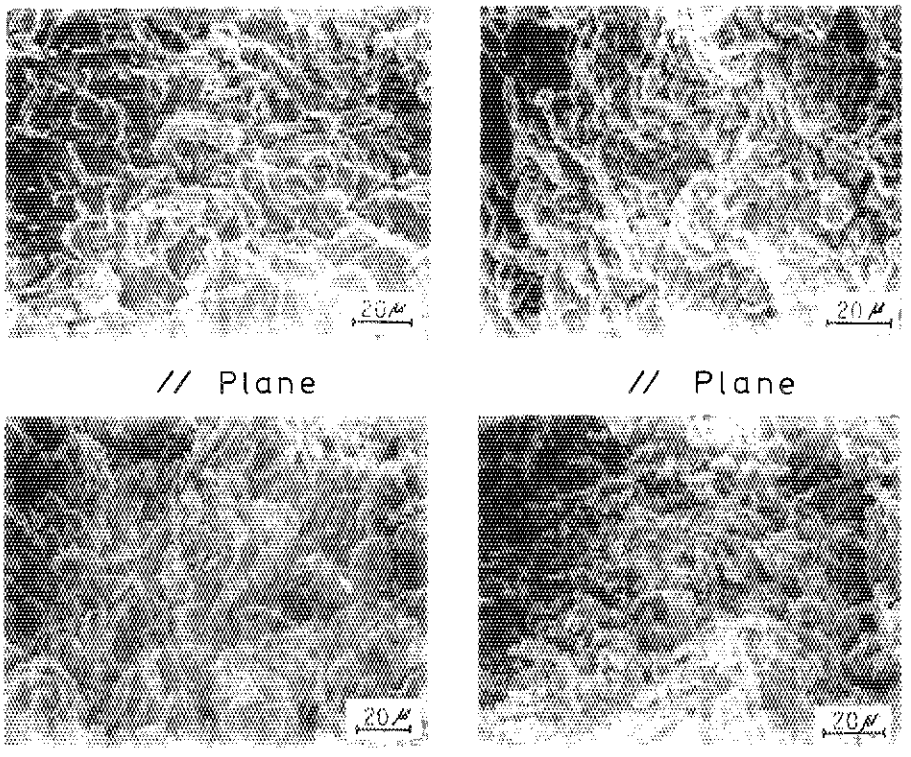

// Plane // Plane

⊥ Plane ⊥ Plane

Sample M4 (NCG) Sample M2 (MICG)

Photo 3 Scanning electron microscope-observations in the fractured faces -planes // (parallel) and ⊥ (perpendicular) to the press direction - of the compact matrixes M2 and M4

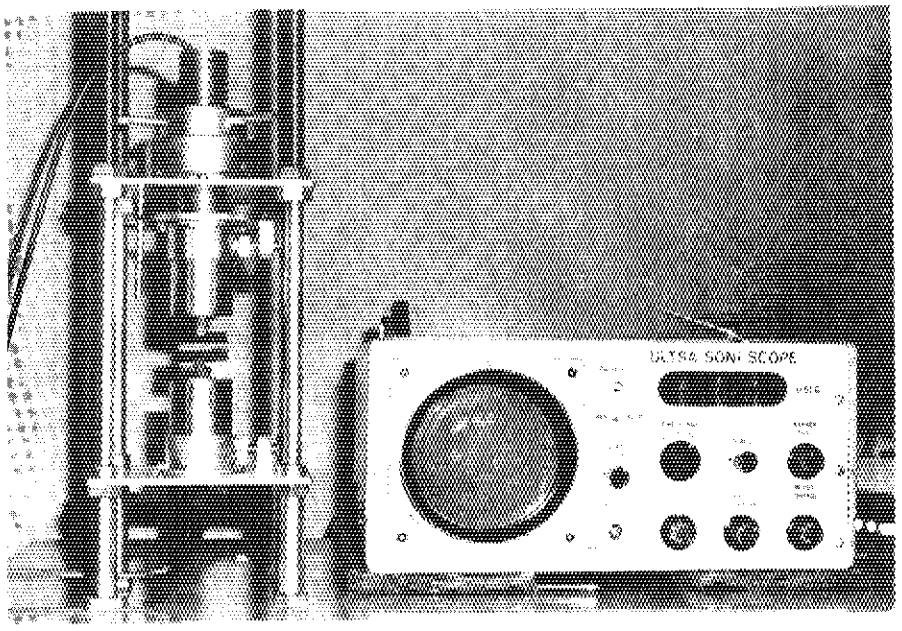

Photo 4 Experimental apparatus -ultrasoniscope(MIN-1105, Marui Co.Ltd.)- for the Young's modulus measurement

Table 3 Reflective intensity ratio obtained by the polarised light method

Sample	Sample No.*1	Observed surface*2	Intensity ratio IR*3	BAF*4
Compact matrix	M2	//	1.06±0.02	1.17
	M2	⊥	1.07±0.02	1.23
	M4	//	1.21±0.02	1.70
	M4	⊥	1.05±0.02	1.17
	M6	//	1.05±0.02	1.17
	M6	⊥	1.09±0.02	1.28
Graphite	7477	//	1.10±0.01	1.33
	IM-2	//	1.06±0.01	1.17

*1 M2 : MICG (Milled isotropic coke graphite) 20 %binder
M4 : NCG (Needle coke graphite) 20 % binder
M6 : PCG (Petroleum coke graphite) 20 % binder
7477 : LeCarbon
IM-2 : AGL

*2 // : Parallel to
⊥ : Perpendicular to
} the press-direction

*3 $IR = r_x/r_z$; r : Reflective intensity

*4 $BAF = 2(1-R_{oz})/R_{oz}$, $R_{oz} = (r_1-r_2)/(r_1-1)(0.5+r_2)$,
$r_1=r_a/r_c=28\%/8\% =3.5$, $r_2=IR$

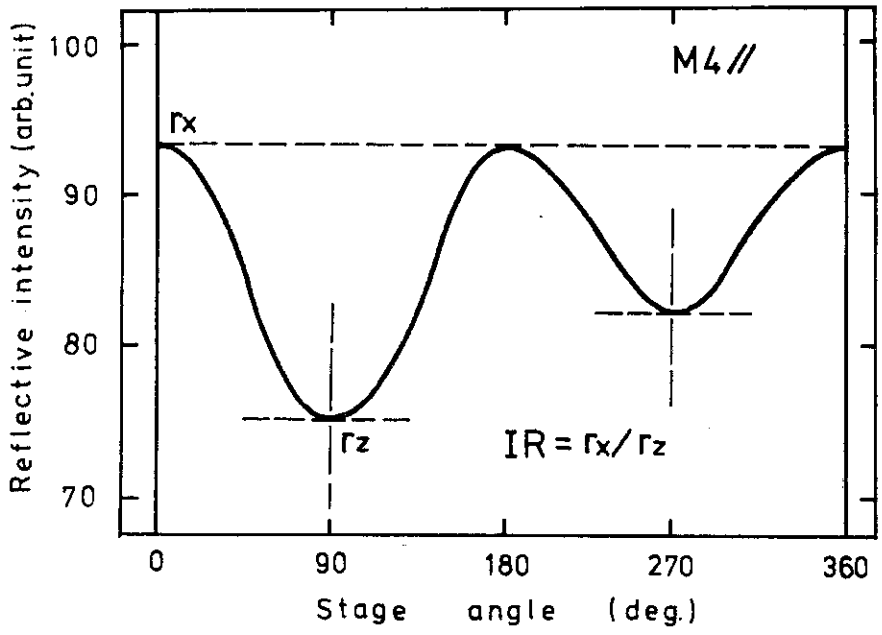

Fig.3 Change of the reflective intensity with the rotation of stage in the compact matrix M4 and the definition of intensity ratio IR

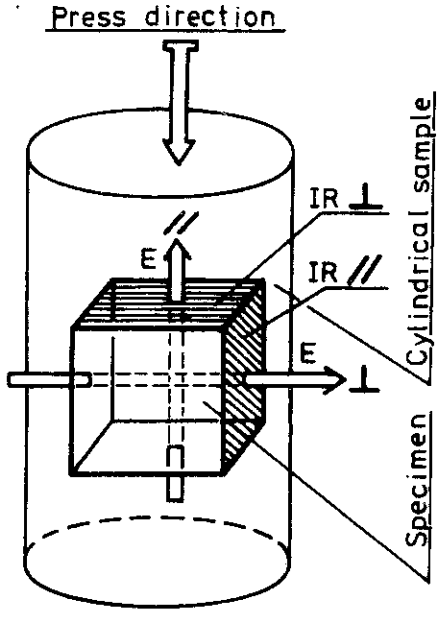

Fig.4 Explanation of the measure-ring directions of Young's modulus E and reflective intensity ratio IR

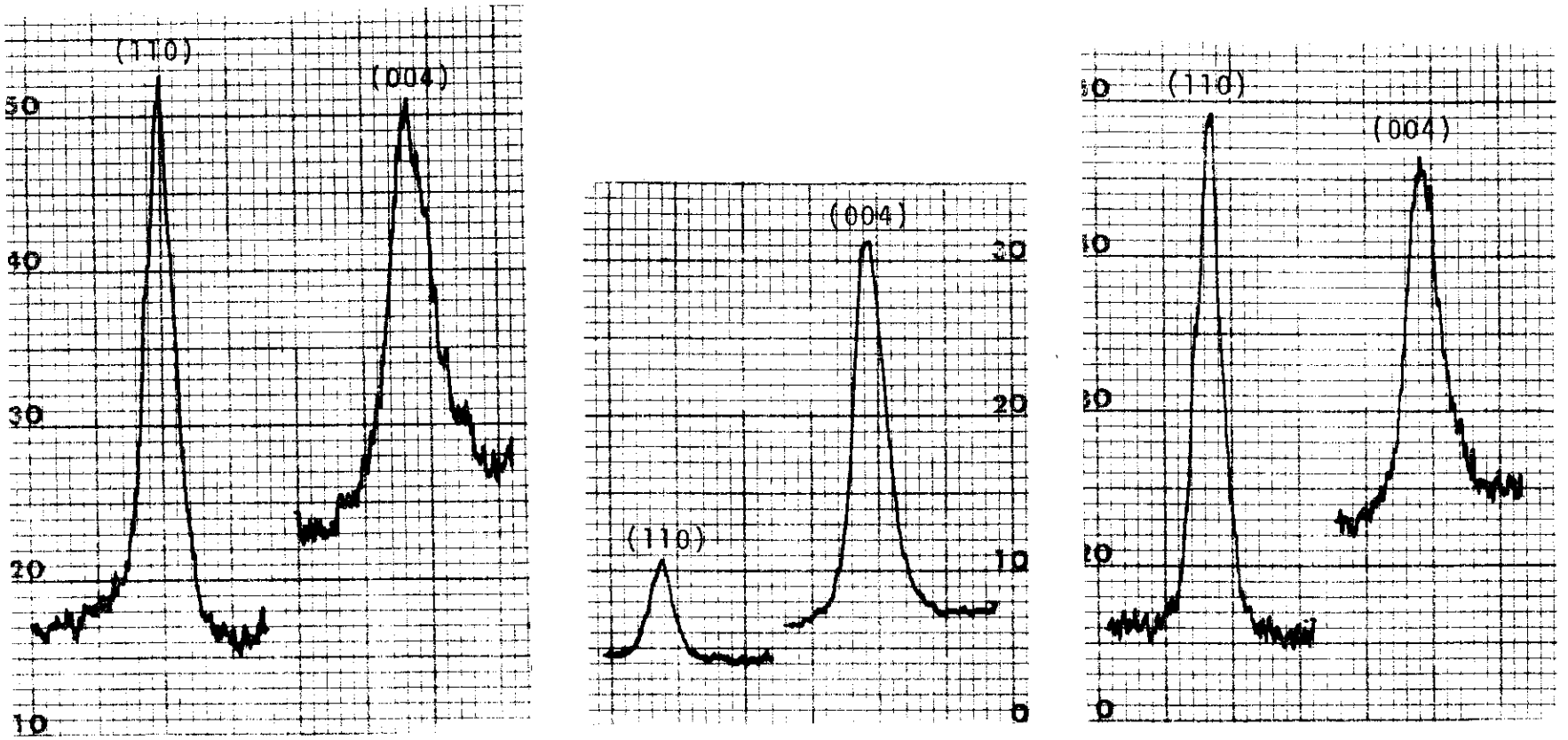

Sample M1 (MICG,10,⊥)　　Sample M3 (NCG,10,//)　　Sample M3 (NCG,10,⊥)

Fig. 5　Typical X ray diffraction patterns in the compact matrices M1 and M3

(MICG:Milled isotropic coke graphite, NCG:Needle coke graphite ;
10 and 20:Contents of phenol resin binder, ⊥ and // :Measurering surfaces)

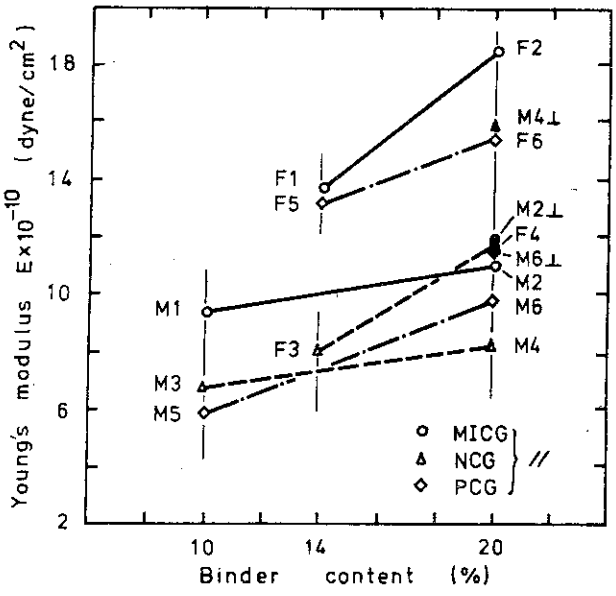

Fig.6 Young's modulus vs. binder content in the compact matrices (M) and the fuel compacts (F)

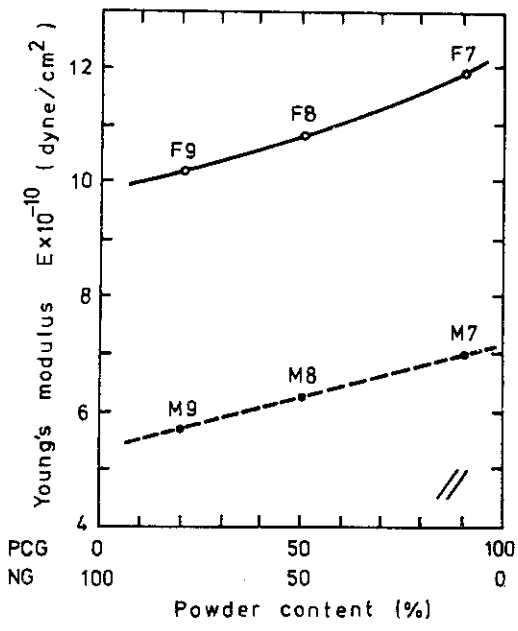

Fig.7 Young's modulus vs. graphite powder content of the compact matrices (M) and the fuel compacts (F) in PCG-NG-system

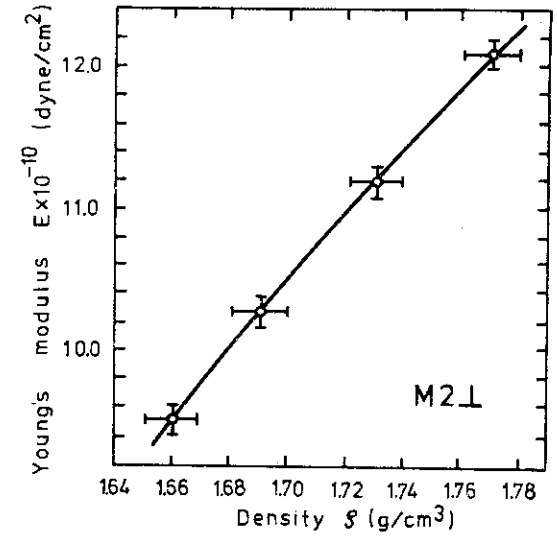

Fig.8 Young's modulus vs. density in the specimens from the compact matrix M2

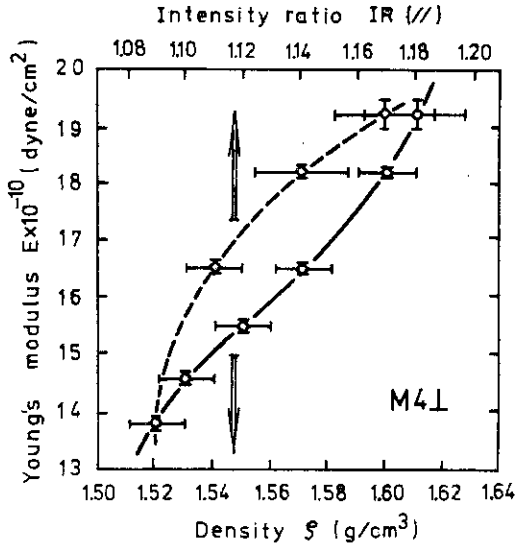

Fig.9 Young's modulus vs. density and reflective intensity ratio in the specimens from the compact matrix M4

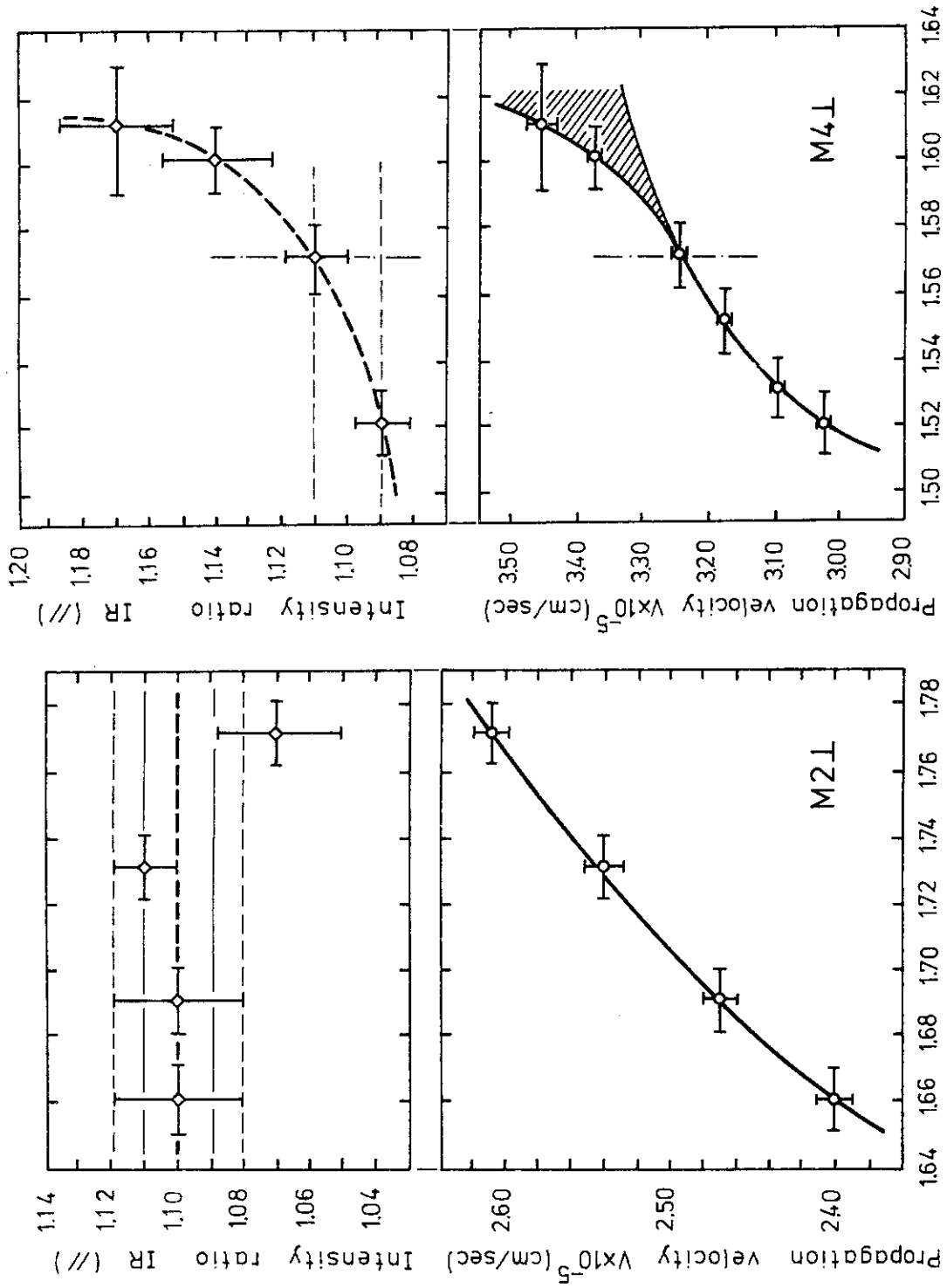

Fig.10 Comparision between the compact matrices M2 and M4 on the reflective intensity ratio and the propagation velocity against density

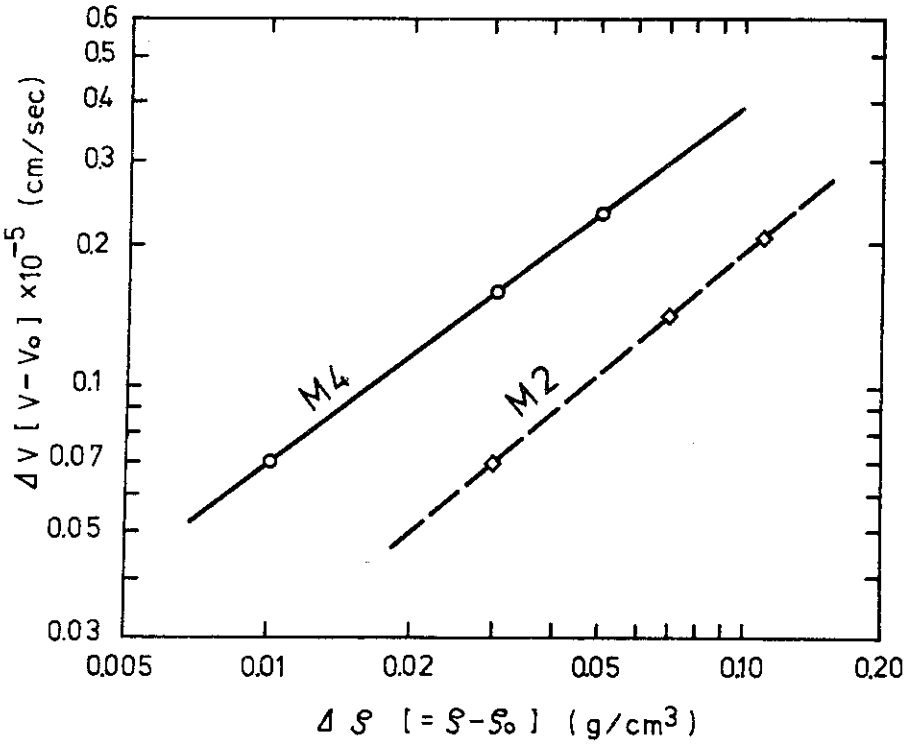

Fig.11 Relation between the increments of density (ρ) and propagation velocity (V) in the compact matrixes M2 and M4

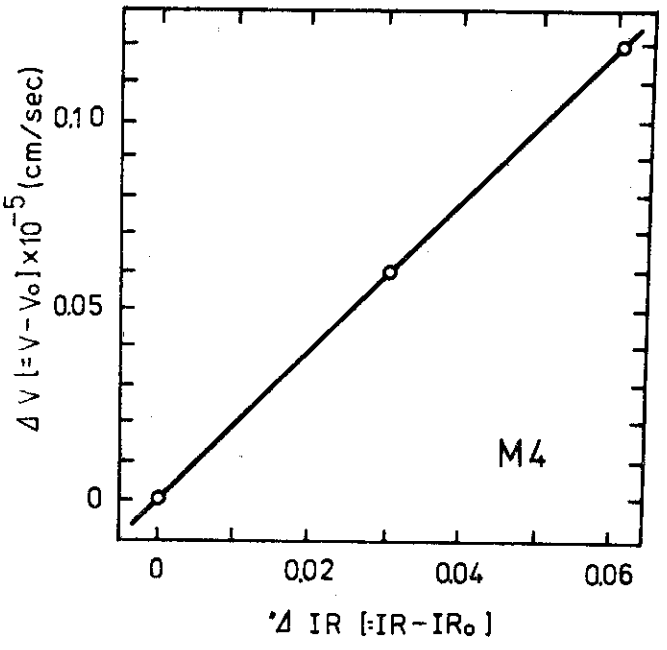

Fig.12 Relation between the increments of reflective intensity ratio (IR) and propagation velocity (V) in the compact matrix M4